AD-A031 226 WASHINGTON UNIV SEATTLE DEPT OF MECHANICAL ENGINEERING F/G 20/11
DYNAMIC FINITE ELEMENT AND DYNAMIC PHOTOELASTIC ANALYSES OF AN --ETC(U)
SEP 76 A S KOBAYASHI, S MALL, A F EMERY N00014-76-C-0060
UNCLASSIFIED TR-26 NL

1 OF 1
ADA031226

END

DATE
FILMED
11 -76

Office of Naval Research

Contract N00014-76-C-0060 NR 064-478

Technical Report No. 26

DYNAMIC FINITE ELEMENT AND DYNAMIC PHOTOELASTIC ANALYSES OF AN IMPACTED PRETENSIONED PLATE

by

A.S. Kobayashi, S. Mall and A.F. Emery

September 1976

The research reported in this technical report was made possible through support extended to the Department of Mechanical Engineering, University of Washington, by the Office of Naval Research under Contract N00014-76-C-0060 NR 064-478. Reproduction in whole or in part is permitted for any purpose of the United States Government.

Department of Mechanical Engineering

College of Engineering

University of Washington

DYNAMIC FINITE ELEMENT AND DYNAMIC PHOTOELASTIC ANALYSES OF AN IMPACTED PRETENSIONED PLATE

by

A.S. Kobayashi, S. Mall and A.F. Emery

ABSTRACT

Dynamic finite element and dynamic photoelasticity were used to analyze ESSO type fracture toughness specimen machined from Homalite-100 sheets of 9.5mm thickness. Crack velocities determined from photoelasticity experiments were prescribed in the dynamic finite element analysis for the purpose of establishing numerically a dynamic fracture toughness which varies with the crack velocity. Qualitative agreement between dynamic energy release rates determined by the two procedures were found, provided an appropriate impulse was prescribed in the dynamic finite element analysis. The dynamic finite element analysis also provided results with sufficient time resolution to confirm our postulate that $K_d = K_c$ at the onset of crack propagation in Homalite-100 plates and that K_a varies in these test specimens.

INTRODUCTION

Two popular test specimens used in studying crack arrest potential of structure steel are the ESSO and Robertson specimens [1,2]* in which dynamic crack propagation is initiated through impacting a wedge in the crack of a subcritically loaded single-edged notch tension plate. Crack arrest in these experiments is attained at regions of either higher fracture toughness generated by higher local temperature in low carbon steel specimen and/or lower stress intensity factors generated by lower local stress field.

---

* Denotes references at the end of this paper.

Previous dynamic photoelastic analysis of ESSO type test specimens modeled by Homalite-100 plates [3] showed that the dynamic effects of the propagating crack combined with that of the impacting projectile have considerable effect on the dynamic stress intensity factor and hence on crack propagation. Unfortunately, these results neither provided a unique relation between the crack velocity and dynamic fracture toughness nor an insight into the basic mechanism of crack arrest. In addition, the results are not in complete agreement with the more recent experimental results obtained on thicker Homalite-100 plates [4,5].

In order to verify, by an independent procedure, some of the controversial results obtained during our past seven-year efforts in fracture dynamics, the authors have used a relatively simple dynamic finite element code to duplicate some of their past work in dynamic photoelasticity [6,7,8]. Encouraged by the reasonable agreements between the numerical and experimental results obtained through this series of studies involving single-edged notch specimens loaded to criticality, the same dynamic finite element code was used to analyze the previous dynamic photoelastic results on the ESSO type test specimens [3].

DYNAMIC PHOTOELASTIC ANALYSIS

The dynamic photoelastic experiments in this paper involve subcritically loaded single-edged notch tension specimens where crack propagation was initiated by an impacted flat-nosed projectile or a 65° wedge. The test specimens consisted of a 9.53mm (3/8 in.) thick Homalite-100 plate with a 0.254 x 0.254m (10 in. x 10 in.) test section loaded in a fixed gripped condition with uniform grip displacement, and with a single-edged starter crack approximately 9.53mm (3/8 in.) in length. The dynamic properties of Homalite-100 were obtained following the procedure of Clark and Sanford [9], which yielded an average dynamic modulus of

of elasticity, Poisson's ratio and stress optic coefficient of 4650 N/mm^2 (675 ksi), 0.345 and 27.2 N/mm^2 fringe (155 psi-in/fringe), respectively. The averaged static fracture toughness, which was obtained through separate tests using SEN specimens, was 20.1 $N/mm^{3/2}$ (579 $psi\sqrt{in}$).

Figure 1 shows 15 frames (1 frame misfired) of dynamic photoelastic patterns obtained by impacting a subcritically loaded single-edged crack plate with a flat nose projectile from the bottom. Note that the crack propagated along a curved path indicating that the crack was driven by the stress waves generated by the impact on this subcritically loaded plate.

Dynamic stress intensity factors, K_D, were determined by Bradley's two parameter procedure [10] and the dynamic energy release rate, $\mathcal{G}_D$, was computed using Freund's equation [11] from the dynamic stress intensity factors. Further details of these data reduction schemes can be found in References 6 and 8.

DYNAMIC FINITE ELEMENT ANALYSIS

The dynamic finite element code, HONDO [12], used in this investigation is based on on explicit time integration scheme and constant strain quadrilateral elements. The crack tip motion was modeled by discontinuous jumps where the crack tip moved from one finite element node to another at discrete time intervals. This discrete propagation of the crack tip generated significant oscillations in the states of stress and displacement surrounding the crack tip. The numerical noise was filtered by computing directly the dynamic energy released by the discrete crack tip advancement from the time-averaged normal stress ahead of the advancing crack tip and the corresponding time-averaged crack opening displacement after crack advance. Details of this numerical procedure as well as an accuracy check of the procedure are described in Reference 6.

Figure 2 shows the finite element breakdown involving a total of 532 elements

and 585 nodes used in this analysis. Impacted wedge-loading was simulated by two simultaneously applied vertical and horizontal forces at the crack mouth without the wedge-shape and the impact forces for the flat nose projectile and 65° wedge were assumed to vary with impact duration. Large plastic deformations at the impact sites were assumed to dissipate about 66 percent and 43 percent of the impact energies for the flat nose and 65° wedge impacts, respectively. Estimates of these energy losses as well as impact durations were made by comparing the calculated dynamic maximum shear stress patterns of a given impulse with the associated dynamic isochromatic patterns along the plate axis of symmetry as shown in Figure 3 and the calculated and measured maximum stresses along the free edge of the specimen as shown in Figure 4. Note that Figures 3 and 4 compare the calculated and measured results in the vicinity of the impact point only and thus one could conclude that the agreements are fair in view of the rapid variations in stresses in this region. As shown in Figure 3, the differences between the calculated and measured stresses decrease rapidly away from the impact point and thus better agreement between the two is to be expected in the region removed from the impact point.

PRETENSIONED SINGLE-EDGED NOTCH PLATE IMPACTED BY FLAT NOSE PROJECTILE

In the series of dynamic photoelastic experiments reported in Reference 3, the crack propagated in some pretensioned single-edged notch plates while it did not run in others. These stop-or-go results potentially provided information for estimating the static fracture toughness under stress-wave loadings but unfortunately the dynamic photoelastic patterns prior to crack propagation were not recorded in these experiments. A combination of dynamic finite element analysis and dynamic photoelasticity results, however, provided a procedure in which the dynamic state prior to the triggering of the dynamic photoelasticity

system could be estimated by some trial and error. Figure 5 shows such variations in dynamic stress intensity factors due to impact for a stationary crack in Test No. W012172 and prior to crack propagation in Test Nos. W020672 and W090771.

It is interesting to note that in Test No. W012172 in which the crack remained stationary the calculated dynamic energy release rate, $\mathcal{G}_D$, is barely equal to or lower than the critical strain energy release rate, $\mathcal{G}_C$. $\mathcal{G}_D$ exceeds $\mathcal{G}_C$ within 20 microseconds after impact and is in agreement with the estimated time at which the crack started to propagate in the dynamic photoelasticity experiments. This combined dynamic photoelasticity-dynamic finite element analysis indicates that the crack initiation dynamic fracture toughness, K_d, under this combined static and stress wave loading is close to, within experimental scatters, the static fracture toughness of K_c = 20.1 N/mm$^{3/2}$ (579 psi$\sqrt{\text{in}}$). Perhaps such coincidence may be expected in view of the recent work by G.C. Smith [13] who found that the variations in fracture toughness of 4.76mm (3/16 in.) thick Homalite-100 plates is approximately equal to the static fracture toughness for the time interval to failure of 20 microseconds. The 30-50 percent increase in stress intensity factor due to impulse loading falls within the rapidly changing dynamic fracture toughness at this time interval to failure.

PRETENSIONED SINGLE-EDGED NOTCH PLATE IMPACTED BY A 65° WEDGE

The dynamic photoelasticity record of Test No. W012472 was analyzed then by the dynamic finite element method using the idealized crack velocity shown in Figure 6. Figure 7 shows the variations in computed dynamic energy release rates due to various impulses used. Figure 8 shows the final impulse used in analyzing this experiment as well as the computed and measured dynamic energy release rates and the computed static strain energy release rate without the

impulse. Momentary crack arrest at a/b $\doteqdot$ 0.39 in the presence of a static strain energy release rate which exceeds $\mathcal{G}_c$ underscores the importance of dynamic analysis in studying the crack arrest phenomenon under such dynamic loading conditions.

DISCUSSIONS

In this study the importance of a correct impulse shape for computing the dynamic energy release rate has been underscored by the sensitivity of dynamic stress intensity factor, K_D, to the varying state of stress which was governed by the applied impulse. Unfortunately, the muzzle velocity measurements of the projectile were unreliable and the subtle variabilities in contact conditions between the projectile and plate appeared to have significant influence on the impulse shape. As a result, considerable amount of trial and error was necessary to arrive at a suitable impulse to match the computed and measured dynamic energy release rates. Such trial and error defeats the original intent of using dynamic finite element method as an independent check of our past dynamic photoelasticity results. Nevertheless, the dynamic finite element analysis served to verify the following.

Our previous conclusion, which was discussed in Reference 7 involving simulated dynamic tear tests, that the fracture toughness at crack initiation did not differ with its static counterpart, appears to be also valid under combined static and impulse loadings. As mentioned previously, these findings are in agreement with those in Reference 13 because of the relatively low strain rate effects involved in these tests.

The dynamic energy release rate at crack arrest was much lower than those measured in non-impact experiments [7] which again reinforces our postulate that $\mathcal{G}_D$ at crack arrest is not a material property. The average dynamic energy release rate, which is obtained by dividing the sum of the total dynamic energy release rates by the newly created crack surface by crack propagation, for Test W012472,

yielded $\mathcal{G}_D]_{ave}/\mathcal{G}_c$ = 2.33 and 2.28 from the dynamic photoelasticity and dynamic FEM analysis, respectively. The large $\mathcal{G}_D]_{ave}$ generated by elastic analysis for a prescribed crack propagation history probably indicates the larger dissipation in dynamic energy due to viscous damping and at the flexible edge grips under high impact loading.

ACKNOWLEDGEMENT

The results reported in this paper were obtained in a research contract funded by the Office of Naval Research under Contract No. N00014-76-C-0060 NR 064-478. The authors wish to acknowledge the continuous support and encouragement of Drs. N.R. Perrone and D. Mulville of ONR.

REFERENCES

1. BLUHM, J.L., Fracture, ed. H. Liebowitz, Vol. V., Academic Press, 1969, 1-63.
2. KANAZAWA, T., Dynamic Crack Propagation, ed. G.C. Sih, Noordhoff International, 1973, 565-597.
3. KOBAYASHI, A.S. and WADE, B.G., ibid loc cit, 663-677.
4. KOBAYASHI, T. and FOURNEY, W.L., Proc. of 12th Annual Meeting of the Society of Engineering Sciences, Univ. of Texas at Austin, Oct. 20-22, 1975.
5. KOBAYASHI, T. and DALLY, J.W., "The Relation Between Crack Velocity and the Stress Intensity Factor in Birefringent Polymers," presented at ASTM Symposium on Fast Fracture and Crack Arrest, Chicago, Illinois, June 28-30, 1976. To be published in ASTM STP.
6. KOBAYASHI, A.S., EMERY, A.F. and MALL, S., "Dynamic Finite Element and Dynamic Photoelastic Analyses of Two Fracturing Homalite-100 Plates," to be published in Experimental Mechanics.
7. KOBAYASHI, A.S. and MALL, S., Proc. of the Int. Conf. on Dynamic Fracture Toughness, London, July 5-7, 1976, 259-272.
8. KOBAYASHI, A.S., EMERY, A.F. and MALL, S., presented at the ASTM Symposium on Fast Fracture and Crack Arrest, Chicago, Illinois, June 28-30, 1976. To be published in ASTM STP.
9. CLARK, A.B.J. and SANFORD, R.J., Proc. of the Soc. for Experimental Stress Analysis, Vol. 20, No. 2, 1973, 148-151.
10. BRADLEY, W.B. and KOBAYASHI, A.S., Engineering Fracture Mechanics, Vol. 3, 1971, 317-332.
11. FREUND, L.B., J. of Mechanics and Physics of Solids, Vol. 20, 1972, 141-152.
12. KEYS, S.W., Sandia Laboratories Report SLA-74-0039, April 1974.
13. SMITH, G.C., PhD Thesis submitted to California Institute of Technology, April 1975.

Figure 1. Dynamic Photoelastic Patterns of a Propagating Crack in a Single-Edged Crack Pretensioned Plate Impacted by a Flat Nose Projectile. Test No. WO90771 Crack missed the 3.8 mm dia. hole located at the center of the plate.

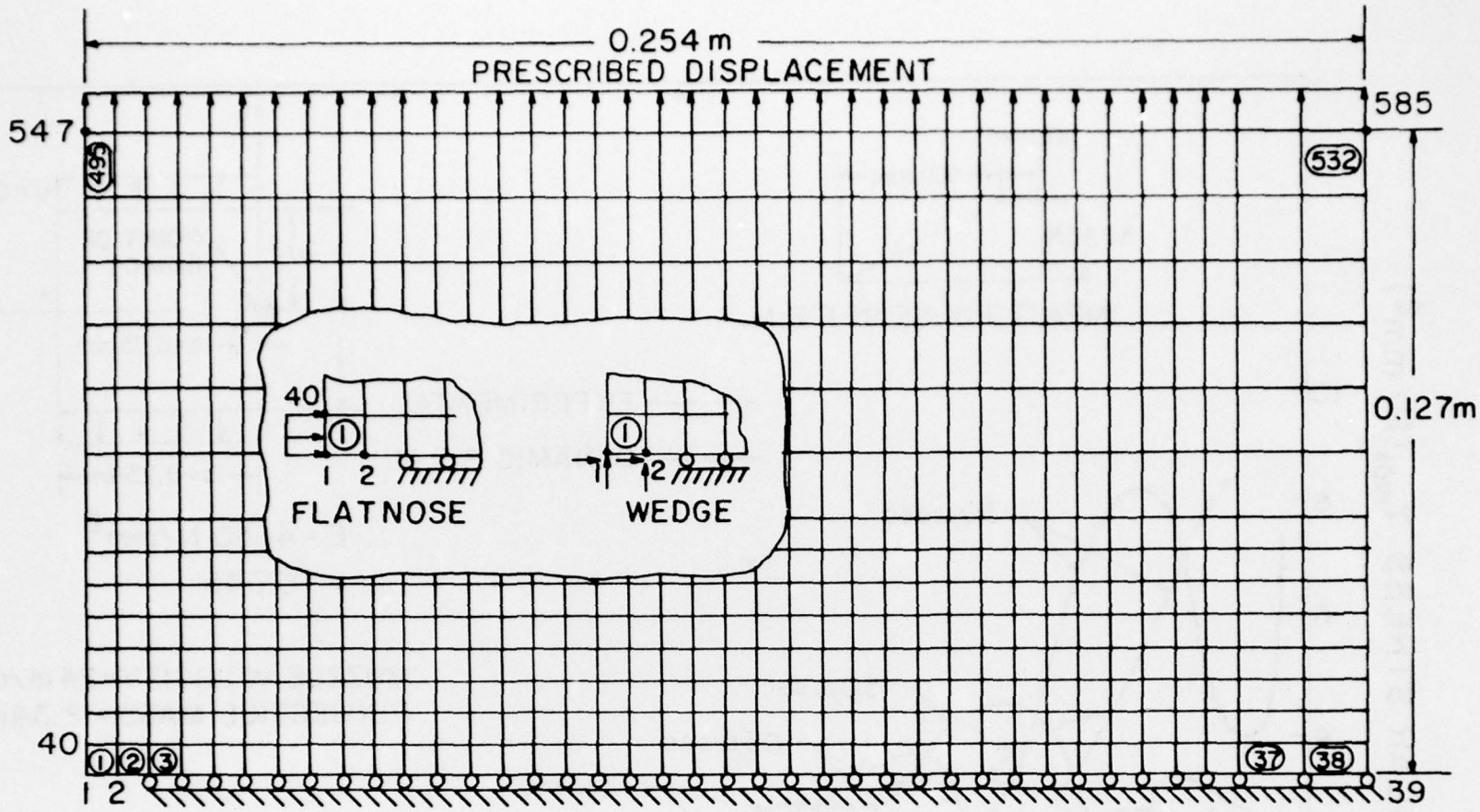

FIGURE 2. FINITE ELEMENT BREAKDOWN WITH APPLIED IMPACT FORCES IN FLATNOSE AND 65° WEDGE PROJECTILE.

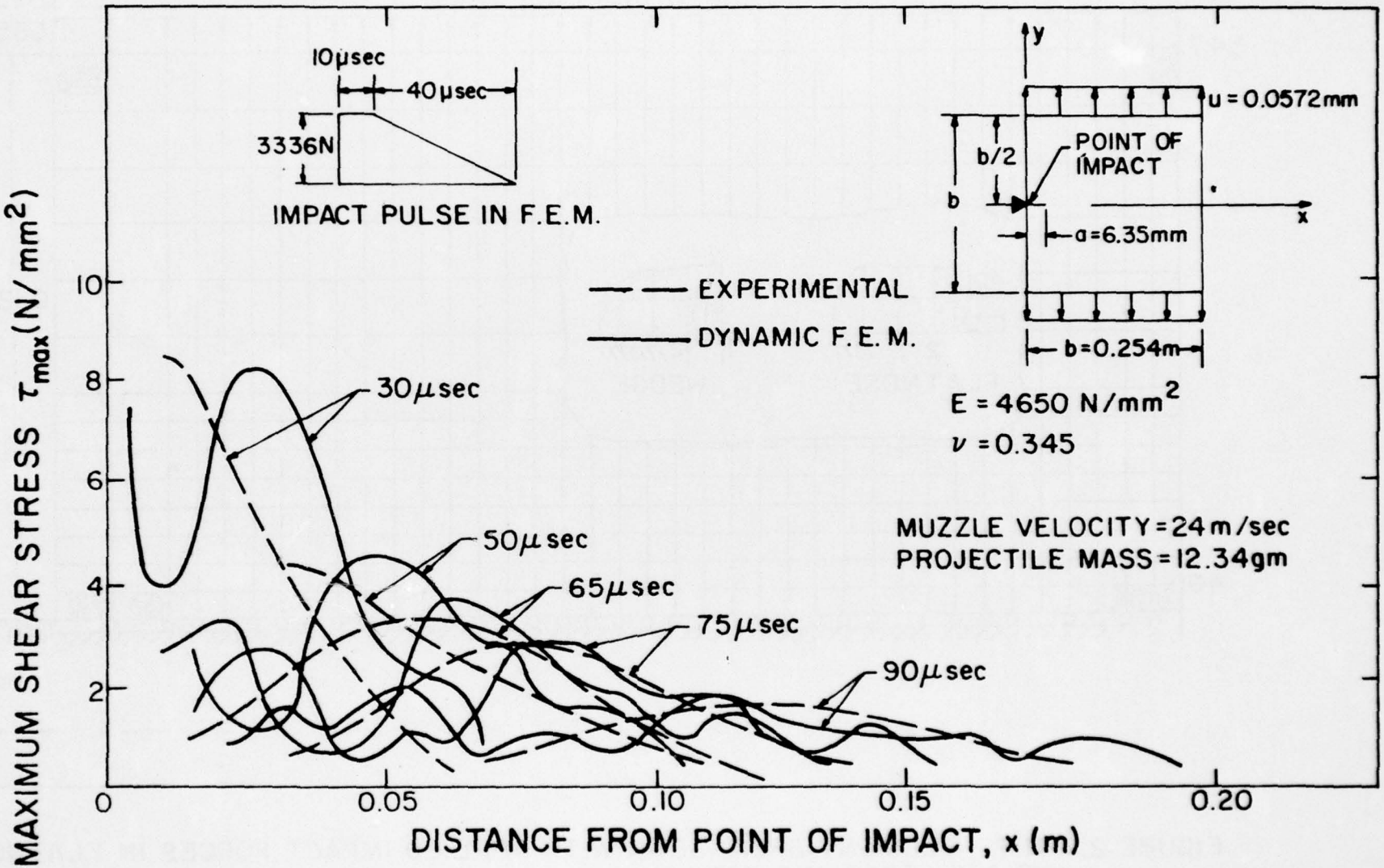

FIGURE 3. DYNAMIC MAXIMUM SHEAR STRESSES ALONG THE AXIS OF SYMMETRY IN SINGLE-EDGED CRACK PRETENSIONED PLATE IMPACTED BY A FLATNOSE PROJECTILE, TEST NO. W012172

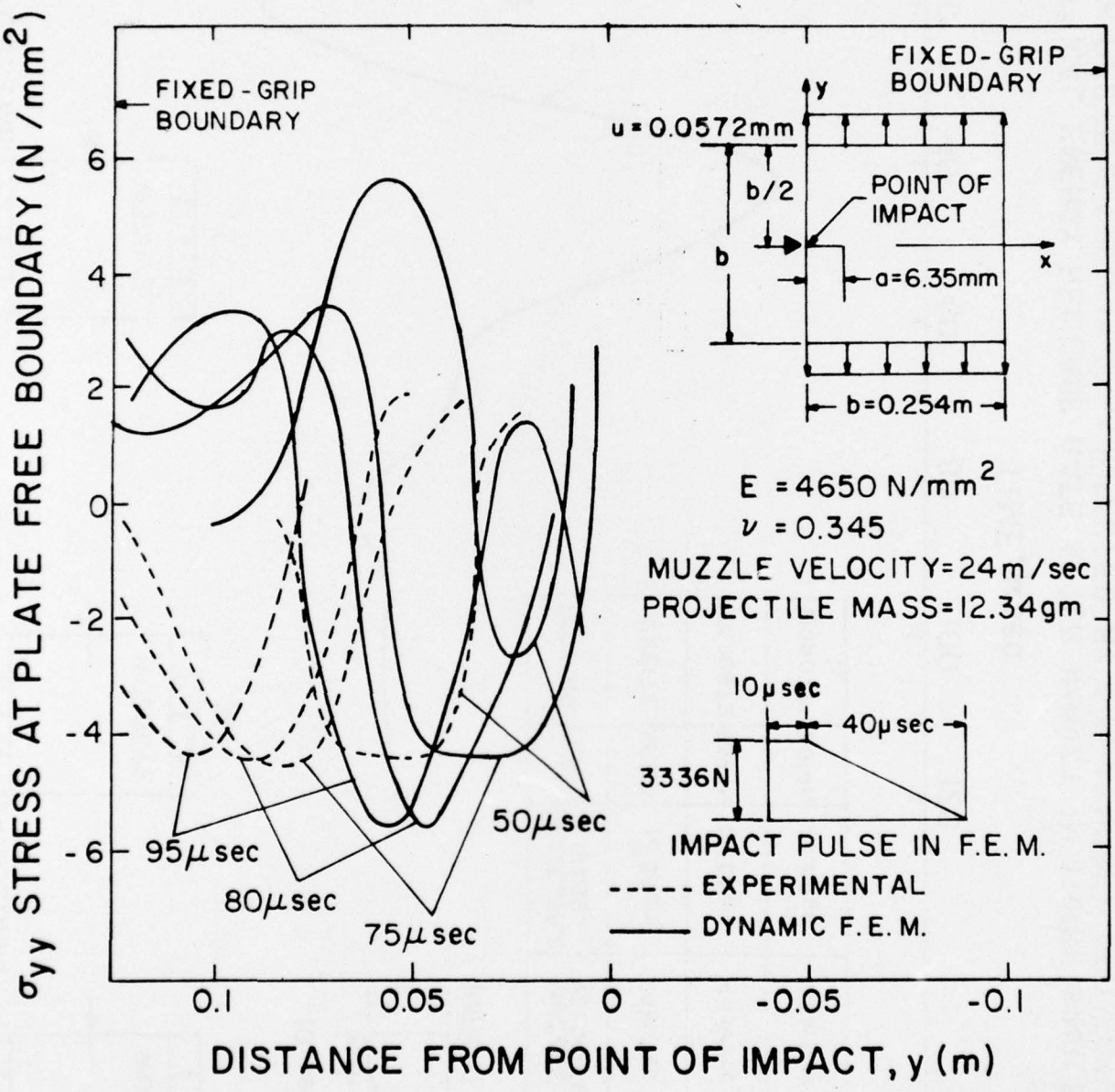

FIGURE 4. DYNAMIC MAXIMUM STRESS, σ_{yy}, ALONG A FREE BOUNDARY IN SINGLE-EDGED CRACK PRETENSIONED PLATE IMPACTED BY A FLATNOSE PROJECTILE, TEST NO. W012172.

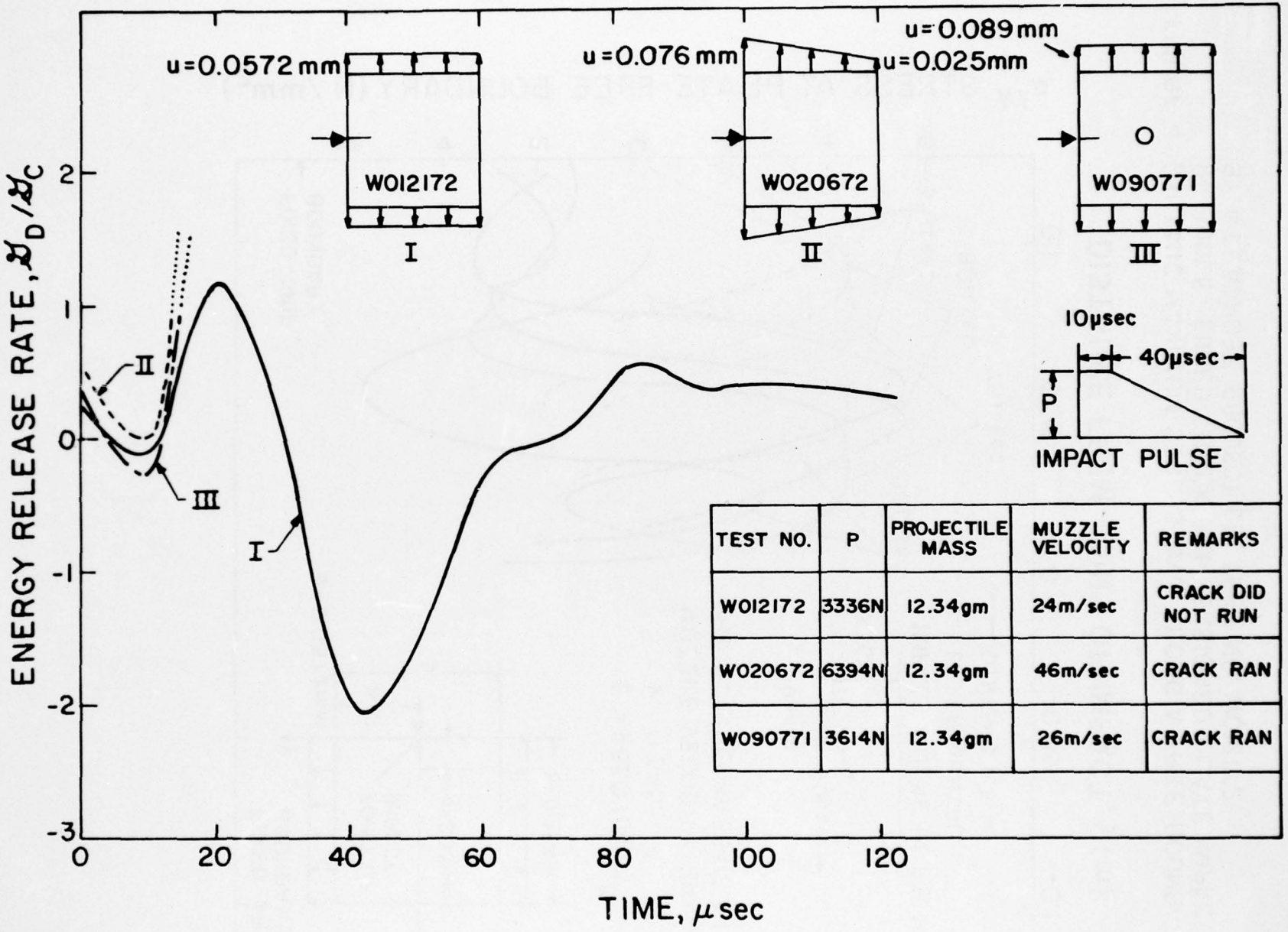

TEST NO.	P	PROJECTILE MASS	MUZZLE VELOCITY	REMARKS
W012172	3336N	12.34gm	24m/sec	CRACK DID NOT RUN
W020672	6394N	12.34gm	46m/sec	CRACK RAN
W090771	3614N	12.34gm	26m/sec	CRACK RAN

FIGURE 5. NUMERICAL ENERGY RELEASE RATE AFTER IMPACT IN THREE SINGLE-EDGED CRACK PRETENSIONED PLATES IMPACTED BY A FLATNOSED PROJECTILE.

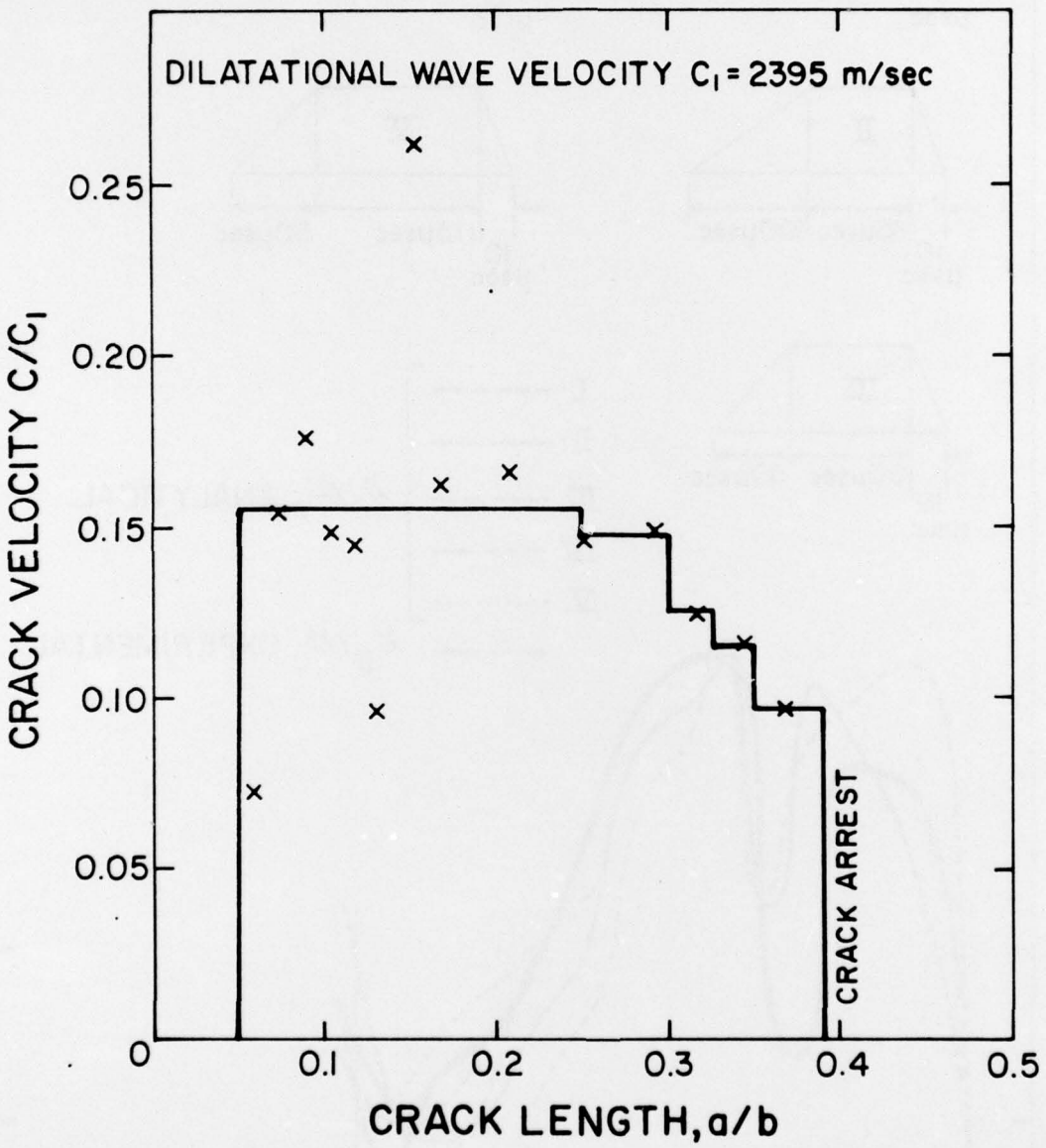

FIGURE 6. CRACK VELOCITIES USED FOR NUMERICAL ANALYSIS ALONG WITH EXPERIMENTAL DATA, TEST NO. W012472

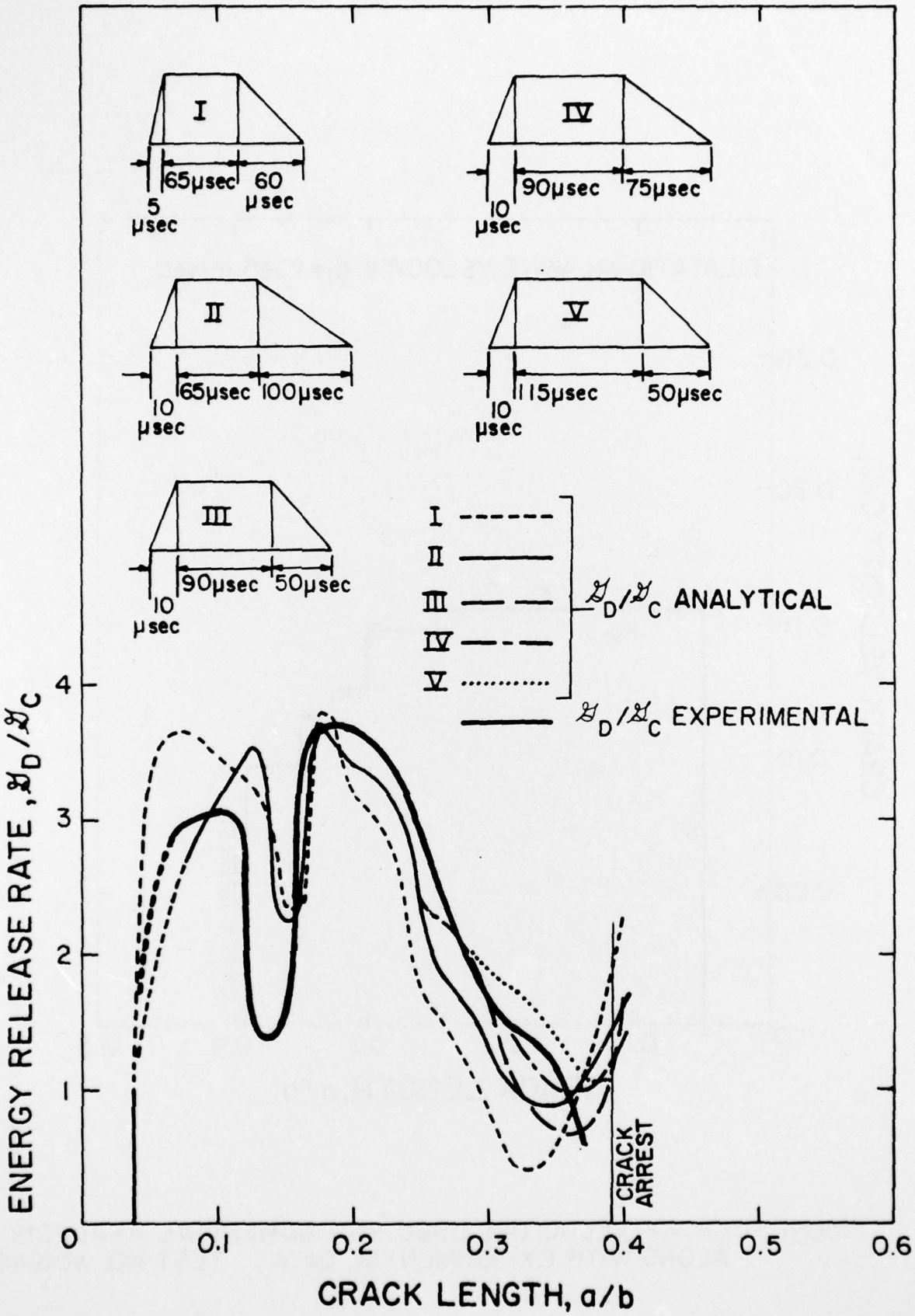

FIGURE 7. ENERGY RELEASE RATES FOR VARIOUS IMPACT PULSES, TEST NO. W012472

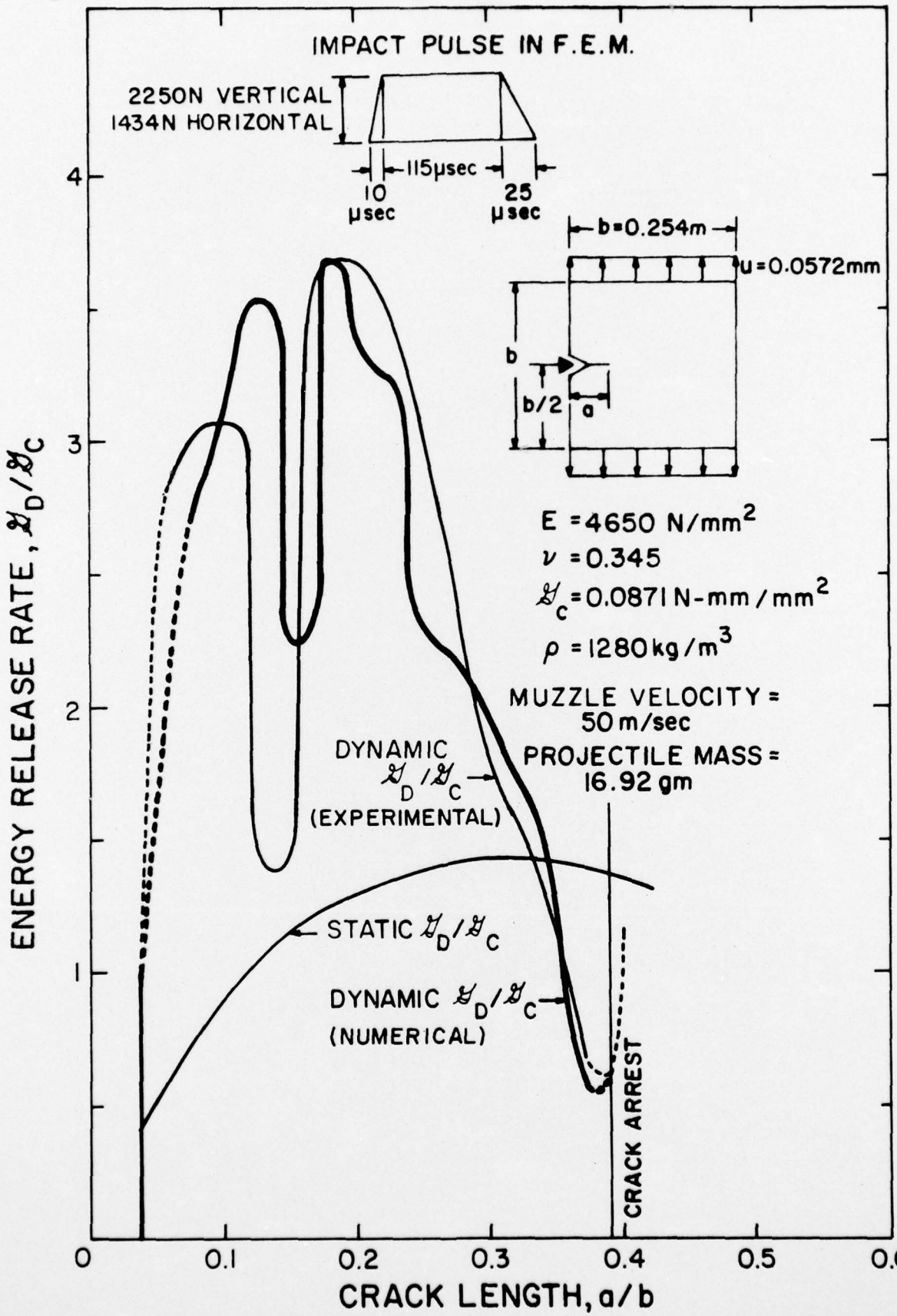

FIGURE 8. ENERGY RELEASE RATES IN A SINGLE-EDGED CRACK PRETENSIONED PLATE IMPACTED BY A 65° WEDGE, TEST NO. W012472

Administrative & Liaison Activities

Chief of Naval Research
Department of the Navy
Arlington, Virginia 22217
Attn: Code 474 (2)
471
222

Director
ONR Branch Office
495 Summer Street
Boston, Massachusetts 02210

Director
Naval Research Laboratory
Attn: Code 2629 (ONRL)
Washington, D.C. 20390 (6)

U.S. Naval Research Laboratory
Attn: Code 2627
Washington, D.C. 20390

Director
ONR - New York Area Office
715 Broadway - 5th Floor
New York, N.Y. 10003

Director
ONR Branch Office
1030 E. Green Street
Pasadena, California 91101

Defense Documentation Center
Cameron Station
Alexandria, Virginia 22314 (12)

Army

Commanding Officer
U.S. Army Research Office Durham
Attn: Mr. J.J. Murray
CRD-AA-IP
Box CM, Duke Station
Durham, North Carolina 27706 (2)

Commanding Officer
AMXMR-ATL
Attn: Mr. R. Shea
US Army Materials Res. Agency
Watertown, Massachusetts 02172

Watervliet Arsenal
MAGGS Research Center
Watervliet, New York 12189
Attn: Director of Research

Techical Library

Redstone Scientific Info. Center
Chief, Document Section
U.S. Army Missile Command
Redstone, Arsenal, Alabama 35809

Army R&D Center
Fort Belvoir, Virginia 22060

Navy

Commanding Officer and Director
Naval Ship Research & Development Center
Bethesda, Maryland 20034
Attn: Code 042 (Tech. Lib. Br.)
17
172
174
177
1800 (Appl. Math. Lab.)
5412S (Dr. W.D. Sette)
19
1901 (Dr. M. Strassberg)
1945
196
1962

Naval Weapons Laboratory
Dahlgren, Virginia 22448

Naval Research Laboratory
Washington, D.C. 20375
Attn: Code 8400
8410
8430
8440
6300
6390
6380

Undersea Explosion Research Div.
Naval Ship R&D Center
Norfolk Naval Shipyard
Portsmouth, Virginia 23709
Attn: Dr. E. Palmer
Code 780

Naval Ship Research & Development Center
Annapolis Division
Annapolis, Maryland 21402
Attn: Code 2740 - Dr. Y.F. Wang
28 - Mr. R.J. Wolfe
281 - Mr. R.B. Niederberger
2814 - Dr. H. Vanderveldt

Technical Library
Naval Underwater Seapons Center
Pasadena Annex
3202 E. Foothill Blvd.
Pasadena, California 91107

U.S. Naval Weapons Center
China Lake, California 93557
Attn: Code 4062 - Mr. W. Werback
4520 - Mr. Ken Bischel

Commanding Officer
U.S. Naval Civil Engt. Lab
Code L31
Port Hueneme, California 93041

Technical Director
U.S. Naval Ordnance Laboratory
White Oak
Silver Spring, Maryland 20910

Technical Director
Naval Undersea R&D Center
San Diego, California 92132

Supervisor of Shipbuilding
U.S. Navy
Newport News, Virginia 23607

Technical Director
Mare Island Naval Shipyard
Vallejo, California 94592

U.S. Navy Underwater Sound Ref. Lab.
Office of Naval Research
PO Box 8337
Orlando, Florida 32806

Chief of Naval Operations
Dept. of the Navy
Washington, D.C. 20350
Attn: Code Op07T

Strategic Systems Project Office
Department of the Navy
Washington, D.C. 20390
Attn: NSP-001 Chief Scientist

Deep Submergence Systems
Naval Ship Systems Command
Code 39522
Department of the Navy
Washington, D.C. 20360

Engineering Dept.
US Naval Academy
Annapolis, Maryland 21402

Naval Air Systems Command
Dept. of the Navy
Washington, D.C. 20360
Attn: NAVAIR 5302 Aero & Structures
5308 Structures
52031F Materials
604 Tech. Library
320B Structures

Director, Aero Mechanics
Naval Air Development Center
Johnsville
Warminster, Pennsylvania 18974

Technical Director
U.S. Naval Undersea R&D Center
San Diego, California 92132

Engineering Department
U.S. Naval Academy
Annapolis, Maryland 21402

Naval Facilities Engineering Command
Dept. of the Navy
Washington, D.C. 20360
Attn: NAVFAC 03 Research & Development
04 " "
14414 Tech. Library

Naval Sea Systems Command
Dept. of the Navy
Washington, D.C. 20360
Attn: NAVSHIP 03 Res. & Technology
031 Ch. Scientist for R&D
03412 Hydromechanics
037 Ship Silencing Div.
035 Weapons Dynamics

Naval Ship Engineering Center
Prince Georges' Plaza
Hyattsville, Maryland 20782
Attn: NAVSEC 6100 Ship Sys. Engr. & Des. Dep.
6102C Computer-Aided Ship Des.
6105G
6110 Ship Concept Design
6120 Hull Div.
6120D Hull Div.
6128 Surface Ship Struct.
6129 Submarine Struct.

Air Force

Commander WADD
Wright-Patterson Air Force Base
Dayton, Ohio 45433
Attn: Code WWRMDD
AFFDL (FDDS)
Structures Division
AFLC (MCEEA)

Chief, Applied Mechanics Group
U.S. Air Force Inst. of Tech.
Wright-Patterson Air Force Base
Dayton, Ohio 45433

Chief, Civil Engineering Branch
WLRC, Research Division
Air Force Weapons Laboratory
Kirtland AFB, New Mexico 87117

Air Force Office of Scientific Research
1400 Wilson Blvd.
Arlington, Virginia 22209
Attn: Mechanics Div.

NASA

Structures Research Division
National Aeronautics & Space Admin.
Langley Research Center
Langley Station
Pimpton, Virginia 23365

National Aeronautic & Space Admin.
Associate Administrator for Advanced
Research & Technology
Washington, D.C. 02546

Scientific & Tech. Info. Facility
NASA Representative (S-AK/DL)
P.O. Box 5700
Bethesda, Maryland 20014

Other Government Activities

Commandant
Chief, Testing & Development Div.
U.S. Coast Guard
1300 E. Street N.W.
Washington, D.C. 20226

Technical Director
Marine Corps Dev. & Educ. Command
Quantico, Virginia 22134

Director
National Bureau of Standards
Washington, D.C. 20234
Attn: Mr. B.L. Wilson, EM 219

Dr. M. Gaus
National Science Foundation
Engineering Division
Washington, D.C. 20550

Science & Tech. Division
Library of Congress
Washington, D.C. 20540

Director
Defense Nuclear Agency
Washington, D.C. 20305
Attn: SPSS

Commander Field Command
Defense Nuclear Agency
Sandia Base
Albuquerque, New Mexico 87115

Director Defense Research & Engrg.
Technical Library
Room 3C-128
The Pentagon
Washington, D.C. 20301

Chief, Airframe & Equipment Branch
FS-120
Office of Flight Standards
Federal Aviation Agency
Washington, D.C. 20553

Chief, Research and Development
Maritime Administration
Washington, D.C. 20235

Deputy Chief, Office of Ship Constrt.
Maritime Administration
Washington, D.C. 20235
Attn: Mr. U.L. Russo

Atomic Energy Commission
Div. of Reactor Devel. & Tech.
Germantown, Maryland 20767

Ship Hull Research Committee
National Research Council
National Academy of Sciences
2101 Constitution Avenue
Washington, D.C. 20418
Attn: Mr. A.R. Lytle

PART 2 - CONTRACTORS AND OTHER TECHNICAL COLLABORATORS

Universities

Dr. J. Tinsley Oden
University of Texas at Austin
345 Eng. Science Bldg.
Austin, Texas 78712

Prof. Julius Miklowitz
California Institute of Technology
Div. of Engineering & Applied Sciences
Pasadena, California 91109

Dr. Harold Liebowitz, Dean
School of Engr. & Applied Science
George Washington University
725 23rd St. N.W.
Washington, D.C. 20006

Prof. Eli Sternberg
California Institute of Technology
Div. of Engr. & Applied Sciences
Pasadena, California 91109

Prof. Paul M. Naghdi
University of California
Div. of Applied Mechanics
Etcheverry Hall
Berkeley, California 94720

Professor P.S. Symonds
Brown University
Division of Engineering
Providence, R.I. 02912

Prof. A.J. Durelli
The Catholic University of America
Civil/Mechanical Engineering
Washington, D.C. 20017

Prof. R.B. Testa
Columbia University
Dept. of Civil Engineering
S.W. Mudd Bldg.
New York, N.Y. 10027

Prof. H.H. Bleich
Columbia University
Dept. of Civil Engineering
Amsterdam & 120th St.
New York, N.Y. 10027

Prof. F.L. DiMaggio
Columbia University
Dept. of Civil Engineering
616 Mudd Building
New York, N.Y. 10027

Prof. A.M. Freudenthal
George Washington University
School of Engineering & Applied Science
Washington, D.C. 20006

D.C. Evans
University of Utah
Computer Science Division
Salt Lake City, Utah 84112

Prof. Norman Jones
Massachusetts Inst. of Technology
Dept. of Naval Architecture & Marine Engineering
Cambridge, Massachusetts 02139

Professor Albert I. King
Biomechanics Research Center
Wayne State University
Detroit, Michigan 48202

Dr. V.R. Hodgson
Wayne State University
School of Medicine
Detroit, Michigan 48202

Dean B.A. Boley
Northwestern University
Technological Institute
2145 Sheridan Road
Evanston, Illinois 60201

Prof. P.G. Hodge, Jr.
University of Minnesota
Dept. of Aerospace Engr. & Mechanics
Minneapolis, Minnesota 55455

Dr. D.C. Drucker
University of Illinois
Dean of Engineering
Urbana, Illinois 61801

Prof. N.M. Newmark
University of Illinois
Dept. of Civil Engineering
Urbana, Illinois 61801

Prof. E. Reissner
University of California, San Diego
Dept. of Applied Mechanics
La Jolla, California 92037

Prof. William A. Nash
University of Massachusetts
Dept. of Mechanics & Aerospace Engr.
Amherst, Massachusetts 01002

Library (Code 0384)
U.S. Naval Postgraduate School
Monterey, California 93940

Prof. Arnold Allentuch
Newark College of Engineering
Dept. of Mechanical Engineering
323 High Street
Newark, New Jersey 07102

Dr. George Herrmann
Stanford University
Dept. of Applied Mechanics
Stanford, California 94305

Prof. J.D. Achenbach
Northwestern University
Dept. of Civil Engineering
Evanston, Illinois 60201

Director, Applied Research Lab.
Pennsylvania State University
P.O. Box 30
State College, Pennsylvania 16801

Prof. Eugen J. Skudrzyk
Pennsylvania State University
Applied Research Laboratory
Dept. of Physics - P.O. Box 30
State College, Pennsylvania 16801

Prof. J. Kempner
Polytechnic Institute of Brooklyn
Dept. of Aero. Engr. & Applied Mech.
333 Jay Street
Brooklyn, N.Y. 11201

Prof. J. Klosner
Polytecnic Institute of Brooklyn
Dept. of Aerospace & Appl. Mech.
333 Jay Street
Brooklyn, N.Y. 11201

Prof. R.A. Schapery
Texas A&M University
Dept. of Civil Engineering
College Station, Texas 77840

Prof. W.D. Pilkey
University of Virginia
Dept. of Aerospace Engineering
Charlottesville, Virginia 22903

Dr. H.G. Schaeffer
University of Maryland
Aerospace Engineering Dept.
College Park, Maryland 20742

Prof. K.D. Willmert
Clarkson College of Technology
Dept. of Mechanical Engineering
Potsdam, N.Y. 13676

Dr. J.A. Stricklin
Texas A&M University
Aerospace Engineering Dept.
College Station, Texas 77843

Dr. L.A. Schmit
University of California, LA
School of Engineering & Applied Science
Los Angeles, California 90024

Dr. H.A. Kamel
The University of Arizona
Aerospace & Mech. Engineering Dept.
Tucson, Arizona 85721

Dr. B.S. Berger
University of Maryland
Dept. of Mechanical Engineering
College Park, Maryland 20742

Prof. G.R. Irwin
Dept. of Mechanical Engineering
University of Maryland
College Park, Maryland 20742

Dr. S.J. Fenves
Carnegie-Mellon University
Dept. of Civil Engineering
Schenley Park
Pittsburgh, Pennsylvania 15213

Dr. Ronald L. Huston
Dept. of Engineering Analysis
Mail Box 112
University of Cincinnati
Cincinnati, Ohio 45221

Prof. George Sih
Dept. of Mechanics
Lehigh University
Bethlehem, Pennsylvania 18015

Prof. A.S. Kobayashi
University of Washington
Dept. of Mechanical Engineering
Seattle, Washington 98195

Librarian
Webb Institute of Naval Architecture
Crescent Beach Road, Glen Cove
Long Island, New York 11542

Prof. Daniel Frederick
Virginia Polytechnic Institute
Dept. of Engineering Mechanics
Blacksburg, Virginia 24061

Prof. A.C. Eringen
Dept. of Aerospace & Mech. Sciences
Princeton University
Princeton, New Jersey 08540

Dr. S.L. Koh
School of Aero., Astro. & Engr. Sci.
Purdue University
Lafayette, Indiana

Prof. E.H. Lee
Div. of Engr. Mechanics
Stanford University
Stanford, California 94305

Prof. R.D. Mindlin
Dept. of Civil Engineering
Columbia University
S.W. Mudd Building
New York, N.Y. 10027

Prof. S.B. Dong
University of California
Dept. of Mechanics
Los Angeles, California 90024

Prof. Burt Paul
University of Pennsylvania
Towne School of Civil & Mech. Engr.
Rm. 113 - Towne Building
220 S. 33rd Street
Philadelphia, Pennsylvania 19104

Prof. H.W. Liu
Dept. of Chemical Engineering & Metall.
Syracuse University
Syracuse, N.Y. 13210

Prof. S. Bodner
Technion R&D Foundation
Haifa, Israel

Prof. R.J.H. Bollard
Chairman, Aeronautical Engr. Dept.
207 Guggenheim Hall
University of Washington
Seattle, Washington 98195

Prof. G.S. Heller
Division of Engineering
Brown University
Providence, Rhode Island 02912

Prof. Werner Goldsmith
Dept. of Mechanical Engineering
Div. of Applied Mechanics
University of California
Berkeley, California 94720

Prof. J.R. Rice
Division of Engineering
Brown University
Providence, Rhode Island 02912

Prof. R.S. Rivlin
Center for the Application of Mathematics
Lehigh University
Bethlehem, Pennsylvania 18015

Library (Code 0384)
U.S. Naval Postgraduate School
Monterey, California 93940

Dr. Francis Cozzarelli
Div. of Interdisciplinary Studies & Research
School of Engineering
State University of New York
Buffalo, N.Y. 14214

Industry and Research Institutes

Library Services Department
Report Section Bldg. 14-14
Argonne National Laboratory
9700 S. Cass Avenue
Argonne, Illinois 60440

Dr. M.C. Junger
Cambridge Acoustical Associates
129 Mount Auburn St.
Cambrige, Massachusetts 02138

Dr. L.H. Chen
General Dynamics Corporation
Electric Boat Division
Groton, Connecticut 06340

Dr. J.E. Greenspon
J.G. Engineering Research Associates
3831 Menlo Drive
Baltimore, Maryland 21215

Dr. S. Batdorf
The Aerospace Corp.
P.O. Box 92957
Los Angeles, California 90009

Dr. K.C. Park
Lockheed Palo Alto Research Laboratory
Dept. 5233, Bldg. 205
3251 Hanover Street
Palo Alto, California 94304

Library
Newport News Shipbuilding and Dry Dock Co.
Newport New, Virginia 23607

Dr. W.F. Bozich
McDonnell Douglas Corporation
5301 Bolsa Ave.
Huntington Beach, California 92647

Dr. H.N. Abramson
Southwest Research Institute
Technical Vice President
Mechanical Sciences
P.O. Drawer 28510
San Antonio, Texas 78284

Dr. R.C. DeHart
Southwest Research Institute
Dept. of Structural Research
PO Drawer 28510
San Antonio, Texas 78284

Dr. M.L. Baron
Weidlinger Associates,
Consulting Engineers
110 East 59th Street
New York, N.Y. 10022

Dr. W.A. von Riesemann
Sandia Laboratories
Sandia Base
Albuquerque, New Mexico 87115

Dr. T.L. Geers
Lockheed Missiles & Space Co.
Palo Alto Research Laboratory
3251 Hanover Street
Palo Alto, California 94304

Dr. J.L. Tocher
Boeing Computer Services, Inc.
P.O. Box 24346
Seattle, Washington 98124

Mr. William Caywood
Code BBE, Applied Physics Laboratory
8621 Georgia Avenue
Silver Spring, Maryland 20034

Mr. P.C. Durup
Lockheed-California Company
Aeromechanics Dept., 74-43
Burbank, California 91503

Addendum:

Assistant Chief for Technology
Office of Naval Research, Code 200
Arlington, Virginia 22217

Unclassified

SECURITY CLASSIFICATION OF THIS PAGE (When Data Entered)

REPORT DOCUMENTATION PAGE		READ INSTRUCTIONS BEFORE COMPLETING FORM
1. REPORT NUMBER 26	2. GOVT ACCESSION NO.	3. RECIPIENT'S CATALOG NUMBER
4. TITLE (and Subtitle) Dynamic Finite Element and Dynamic Photoelastic Analyses of an Impacted Pretensioned Plate		5. TYPE OF REPORT & PERIOD COVERED Interim Report 6. PERFORMING ORG. REPORT NUMBER TR-26
7. AUTHOR(s) A.S. Kobayashi, S. Mall and A.F. Emery		8. CONTRACT OR GRANT NUMBER(s) N00014-76-C-0060 NR 064-478
9. PERFORMING ORGANIZATION NAME AND ADDRESS University of Washington Department of Mechanical Engineering Seattle, Washington 98195		10. PROGRAM ELEMENT, PROJECT, TASK AREA & WORK UNIT NUMBERS
11. CONTROLLING OFFICE NAME AND ADDRESS Office of Naval Research Arlington, Virginia		12. REPORT DATE September 1976 13. NUMBER OF PAGES 15
14. MONITORING AGENCY NAME & ADDRESS(if different from Controlling Office)		15. SECURITY CLASS. (of this report) 15a. DECLASSIFICATION/DOWNGRADING SCHEDULE

16. DISTRIBUTION STATEMENT (of this Report)

Unlimited

DISTRIBUTION STATEMENT A
Approved for public release;
Distribution Unlimited

17. DISTRIBUTION STATEMENT (of the abstract entered in Block 20, if different from Report)

18. SUPPLEMENTARY NOTES

19. KEY WORDS (Continue on reverse side if necessary and identify by block number)

Fracture Mechanics
Crack Propagation
Crack Arrest
Impact
Dynamic Photoelasticity

20. ABSTRACT (Continue on reverse side if necessary and identify by block number)

Dynamic finite element and dynamic photoelasticity were used to analyze ESSO type fracture toughness specimen machined from Homalite-100 sheets of 9.5mm thickness. Crack velocities determined from photoelasticity experiments were prescribed in the dynamic finite element analysis for the purpose of establishing numerically a dynamic fracture toughness which varies with the crack velocity. Qualitative agreement between dynamic energy release rates determined by the two procedures were found, provided an appropriate impulse was prescribed

→ OVER

DD FORM 1 JAN 73 1473 EDITION OF 1 NOV 65 IS OBSOLETE
S/N 0102-014-6601

Unclassified

SECURITY CLASSIFICATION OF THIS PAGE (When Data Entered)

400 344

(Contin. of 20.)

in the dynamic finite element analysis. The dynamic finite element analysis also provided results with sufficient time resolution to confirm our postulage that $K_A = K_B$ at the onset of crack propagation in Homalite-100 plates and that K_A varies in these test specimens.